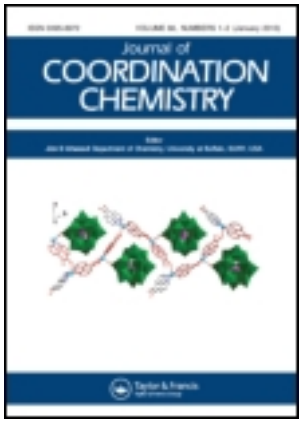


Journal of Coordination Chemistry
Publication details, including instructions for authors and subscription information:
http://www.tandfonline.com/loi/gcoo20

# Copper(II) bis-chelate paddle wheel complex and its bipyridine/phenanthroline adducts

P. Mosae Selvakumar [a], S. Nadella [a], Jashbanta Sahoo [a], E. Suresh [a] & P.S. Subramanian [a]

[a] Analytical Science Division, Central Salt and Marine Chemicals Research Institute, Bhavnagar, India

Accepted author version posted online: 04 Dec 2012.Published online: 21 Jan 2013.

To cite this article: P. Mosae Selvakumar, S. Nadella, Jashbanta Sahoo, E. Suresh & P.S. Subramanian (2013) Copper(II) bis-chelate paddle wheel complex and its bipyridine/phenanthroline adducts, Journal of Coordination Chemistry, 66:2, 287-299, DOI: 10.1080/00958972.2012.755521

To link to this article: http://dx.doi.org/10.1080/00958972.2012.755521

*Journal of Coordination Chemistry*
Vol. 66, No. 2, 20 January 2013, 287–299



# Copper(II) bis-chelate paddle wheel complex and its bipyridine/phenanthroline adducts

P. MOSAE SELVAKUMAR, S. NADELLA, JASHBANTA SAHOO, E. SURESH and P.S. SUBRAMANIAN*

Analytical Science Division, Central Salt and Marine Chemicals Research Institute, Bhavnagar, India

(*Received 23 February 2012; in final form 11 October 2012*)

Bola-shaped diester dicarboxylic acid 2-({2-[(2-carboxybenzoyl)-xy]ethoxy}carbonyl)benzoic acid ($L^1H_2$) was synthesized by desymmetrizing phthalic anhydride using 1,2-ethane diol. The corresponding dinuclear copper(II)-tetracarboxylate complex $[Cu_2(L^1)_2{\cdot}(DMF)_2]$ (**1**) has been synthesized. This paddle wheel complex was self-assembled with *[15]*-membered bis-chelate ring on either sides of the M–M axis. Upon treating with phenanthroline/bipyridine, the symmetrically formed bis-chelate rings in **1** were selectively desymmetrized into monochelate rings. The dinuclear association in **1** rearranged into mononuclear in $[Cu(L^1){\cdot}(bpy)]$ (**2**) and $[Cu(L^1){\cdot}(phen)]{\cdot}(DMF)$ (**3**), where bpy = bipyridine and phen = phenanthroline. The paddle wheel arrangement in **1** is very similar to that in dimeric Cu(II) acetate; the symmetric arrangement in **1** rearranged in its corresponding monomeric species on reacting with phen and bpy. The symmetric bis-chelate ring in **1** and the desymmetrized monochelate ring in **2** and **3** are discussed following their crystal structures. The crystal structures for all the complexes and the electronic and fluorescence properties are discussed.

*Keywords*: Copper; Carboxylate; Paddle wheel; Dimers; Coordination; Bis-chelate



## 1. Introduction

Metal carboxylates [1, 2] have been studied because of the versatile coordination of carboxylate. Ever since the discovery of $[Cu(CH_3COO)_2{\cdot}H_2O]$, a variety of metal acetates were synthesized and characterized with an interest to investigate the Cu–Cu interaction [3–5] or as catalyst for a variety of organic reactions [6, 7]. Cu(II) is an essential bioelement and the ubiquitous presence of dimeric Cu-Cu in many metalloproteins and metalloenzymes [8, 9] deserves paramount importance due to their dimeric to monomeric [10] rearrangement associated with its functional mechanism. Monocarboxylate coordinates [11, 12] as monodentate, bidentate, chelate, *syn-syn*, *syn-anti,* and *anti-anti*. Dicarboxylates and polycarboxylates with flexible aliphatic backbones are expected to adopt various conformational freedoms. Thus, the change in coordination and conformational freedom is expected to play significant roles as building blocks in construction of metal organic frameworks and inorganic–organic hybrid polymeric networks. The mode of coordination of carboxylate plays an important role in mediating M–M interaction, magnetic exchange pathway, electron transfer,

*Corresponding author. Email: siva@csmcri.org


ISSN 0095-8972 print/ISSN 1029-0389 online © 2012 Taylor & Francis
http://dx.doi.org/10.1080/00958972.2012.755521

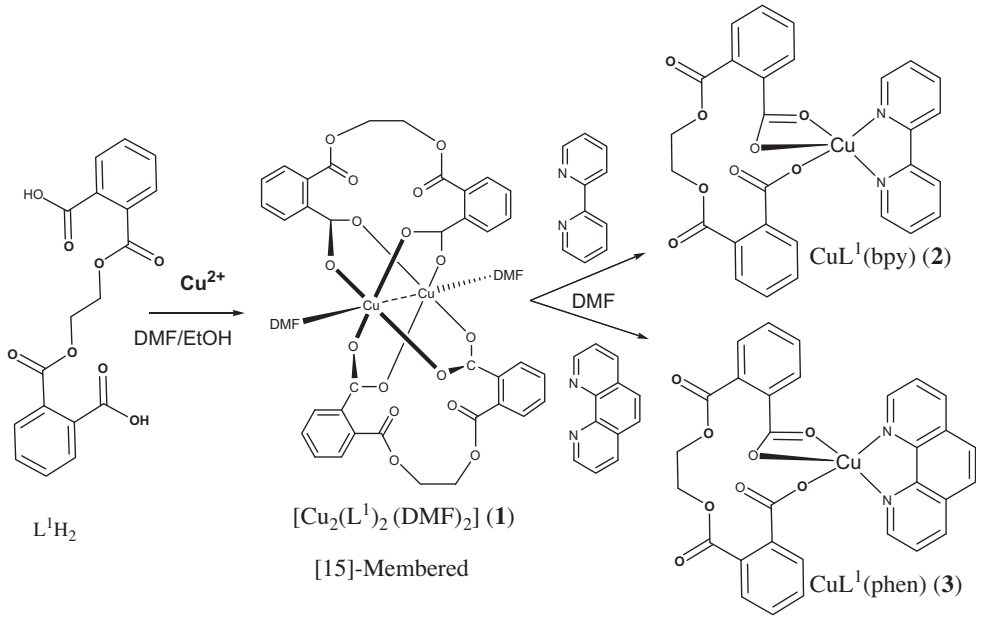


Scheme 1. Synthesis of ligand and complexes.

*etc*. In this regard, parallel to cupric acetate, the "paddle wheel" conformation observed in $[Cu_2(L^1)_2{\cdot}(DMF)_2]$ (**1**) as well as in various other related complexes are of interest. We recently reported a series of dinuclear $Cu_2$ tetracarboxylates [13, 14] with some interesting bis-chelate complexes, similar to that of Bickley *et al*. [15]. In continuation, here, we demonstrate that the symmetric $Cu_2$ dimer selectively desymmetrized into monomer followed by structural rearrangement from bis-chelate ring in **1** into monochelate ring in **2** and **3**, based on their spectral data and single crystal X-ray structures. Terminal carboxylates of $L^1$ in **2** and **3** exhibit an interesting coordination with chelate and monodentate to Cu(II) as shown in scheme 1.

## 2. Experimental

### 2.1. *Materials and methods*

All reagents and solvents were commercially available and used without purification. Elemental analysis was performed on a Perkin-Elmer 4100 elemental analyzer. Fluorescence spectra were recorded on a Perkin-Elmer Luminescence Spectrometer LS 50B. Electronic spectra were recorded on a Shimadzu UV 3101PC spectrophotometer. IR spectra were recorded using KBr pellets on a Perkin-Elmer Spectrum GX FT-IR spectrometer. Mass analyzes were performed using electron spray ionization ($ESI^+$) on a Waters Q Tof-micro mass spectrometer. $^1H$ and $^{13}C$ NMR spectra were recorded (200.16 and 50.3 MHz, respectively) on a BRUKER *Avance* DPX 200 NMR spectrometer.

### 2.2. *Crystal structure determination*

For **1**, **2,** and **3,** a crystal of suitable size was selected and mounted on the tip of a glass fiber and cemented using epoxy resin. Intensity data for the crystals were collected using

Mo-$K_\alpha$ ($\lambda = 0.71073$ Å) radiation on a Bruker SMART APEX diffractometer equipped with a charge coupled device area detector at 100 K. The data integration and reduction were processed with SAINT software. An empirical absorption correction was applied to the collected reflections with SADABS. The structures were solved by direct methods using SHELXTL and refined on $F^2$ by full-matrix least-squares using the SHELXL-97 package [16]. Graphics are generated using PLATON [17] and MERCURY 1.3 [18]. In the complexes, nonhydrogen atoms were refined anisotropically till convergence. Hydrogens in both ligands were fixed at idealized positions stereochemically.



### 2.3. *Synthesis*

**$L^1H_2$**: 2-({2-[(2-carboxybenzoyl)xy]ethoxy}carbonyl)benzoic acid: $L^1H_2$ was synthesized and characterized as per our reported procedure [14]. Yield 75% Anal. Calcd for $C_{18}H_{14}O_8$ (%): C, 60.34; H, 3.94. Found (%): C, 60.12; H, 3.68. MS [$ESI^+$]: Calc for $C_{18}H_{14}O_8$, 381.06 $(M+Na)^+$ Found 381.12. $^1H$ NMR *(Methanol-$D_4$, δ, TMS, 200.16 MHz)*: 7.66(*m*, *Ar*, *2H*), 7.62(*m*, *2H*), 7.58(*m, 4H*), 4.60(*–$CH_2$,4H*). $^{13}C$ NMR [*Methanol-$D_4$, δ, TMS, 50.3 MHz*]: 169.58 (*C=O*), 168.86 (C=O), 132.36, 132.01(*quat-C*), 131.37, 131.05, 129.04, 128.53 (*=CH*), 63 (*–$CH_2$*). IR: (*v*, $cm^{-1}$, KBr); 1723 (st); 1694; 1419; 1315, 1290; 1127, 744.

**[$Cu_2(L^1)_2\cdot(DMF)_2$]** (**1**): $[Cu(CH_3COO)_2]\cdot H_2O$ (0.398 g, 0.002 M) dissolved in 25 mL of DMF was added slowly to ethanolic solution of $L^1H_2$ (0.0716 g, 0.002 mM) and stirred continuously followed by addition of triethylamine (0.004 mM). Color change from greenish blue to dark green was observed indicating complexation. Precipitate was separated, washed with water, and dried. Suitable single crystals were obtained dissolving the precipitate in DMF with slow evaporation at room temperature in three weeks. Yield 78%. Dark green, Anal. Calcd for $C_{42}H_{40}Cu_2N_2O_{18}$ (%): C, 51.06; H, 4.08; N, 2.84. Found (%): C, 51.06; H, 4.08; N, 2.84. MS [$ESI^+$] Calcd for $C_{36}H_{24}Cu_2O_{16}Na$ 862.97(M-2DMF $+Na^+$); Found, 863.18. UV–vis: (DMF, λ, nm, ε) 269(1950), 750(350). IR (*v, $cm^{-1}$*, KBr) 3444, 3069, 2932, 2360, 1955, 1738, 1665, 1624, 1595, 1405, 1284, 1248, 1116, 1081, 1039, 873, 752.

**[Cu($L^1$)·(bpy)]** (**2**): The 1 : 2 ratio of **1** (0.980 g, 0.001 M) and 2,2′-bipyridine (0.312 g, 0.002 M) were mixed and refluxed in 25 mL of DMF for 3 h at 80 °C. Color change from green to blue indicated complexation. The resultant solution was kept for crystallization. Suitable single crystals were obtained from the solution upon slow evaporation at room temperature in four weeks. Yield 72%. Blue, Anal. Calcd for $C_{28}H_{20}CuN_2O_8$ (%): C, 58.38; H, 3.84; N, 4.85. Found (%): C, 58.16; H, 3.42; N, 4.89. MS [$ESI^+$] Calcd for $C_{28}H_{20}CuN_2O_8$, 598.04($M+Na^+$), 575.05($M+H^+$); Found: 598.40, 576.15. UV–vis: (DMF, λ, nm, ε) 275(1980), 650(098). IR (*v, $cm^{-1}$*, KBr) 3428, 3063, 3038, 2997, 2360, 1725, 1634, 1602, 1553, 1568, 1448, 1401, 1362, 1279, 1250, 1156, 1112, 1076, 1034, 858, 762.

**[Cu($L^1$)·(phen)]·DMF** (**3**): The above procedure for **2** was repeated with 1,10-phenanthroline monohydrate used in place of 2,2′-bipyridine. Yield 75%. Blue. MS [$ESI^+$] Calcd for $C_{30}H_{20}CuN_2O_8$ 599.05($M+H^+$), 622.04($M+Na^+$), 638.02(($M+K^+$), Found: 600.16, 622.11, 638. Anal data Calcd for $C_{33}H_{27}CuN_3O_9$: C, 58.88; H, 4.04; N, 6.24%. Found: C, 58.74; H, 3.94; N, 6.11%; UV–vis (DMF, λ, nm, ε): 270(1950), 648(100). IR (*v, $cm^{-1}$*, KBr) 3469, 3061, 2954, 2360, 1729, 1621, 1590, 1568, 1519, 1427, 1369, 1285, 1249, 1150, 1117, 1076, 1039, 855, 773.

## 3. Results and discussion

The bola-shaped diester-dicarboxylic acid $L^1H_2$ with 1,2-ethanediol spacer and aromatic head groups was synthesized following our reported procedure [14]. Using 1 : 1 $L^1H_2$ Cu (II) ratio dissolved in ethanol/DMF mixture, a binuclear $Cu^{II}$-tetracarboxylate $[Cu_2(L^1)_2{\cdot}(DMF)_2]$ (**1**) was synthesized as shown in scheme 1. $L^1H_2$ self-assembled into the tetracarboxylate dinuclear Cu(II) bis-chelate complex $[Cu_2(L^1)_2{\cdot}(DMF)_2]$. As shown in scheme 1, treating **1** with 2,2′-bpy and 1,10-phen, the symmetric bis-chelate rings are desymmetrized into monochelate rings in **2** and **3** with rearrangement of the carboxylate coordination. Single crystals suitable for X-ray diffraction for all three complexes were obtained from ethanol: DMF solvent mixture upon slow evaporation at room temperature.



### 3.1. *IR spectra*

IR spectra for these Cu(II) complexes and $L^1H_2$ were recorded as KBr disks. The free ligand gives two easily distinguishable intense peaks attributable to $\nu_{asym}(COO^-)$ and $\nu_{sym}(COO^-)$. Broad and intense bands at 1720 and 1690 $cm^{-1}$ reflect the small difference between the asymmetric and symmetric stretch of the carboxylic acid. The dinuclear Cu(II) complexes **1–3** possess two sets of peaks distinguishable to terminal and spacer carboxylates, representing coordinated and noncoordinated forms from 1750 to 1400 $cm^{-1}$. Strong and intense peaks at 1715–1723 $cm^{-1}$ and 1627–1633 $cm^{-1}$ are attributed to symmetric and asymmetric stretch of the noncoordinated carboxylic acid, while signals at 1593–1595 $cm^{-1}$ and 1401–1404 $cm^{-1}$ match well with coordinated terminal carboxylate. The $\Delta\nu[\nu_{asym}COO^- - \nu_{sym}COO^-]$ for spacer carboxylates of $90 \pm 5$ $cm^{-1}$ indicates that $\nu_{sym}COO^-$ has shifted to lower wave number. This shift in the asymmetry stretching mode for **1–3** indicates that the spacer moiety is involved in some weak interaction in the solid state. The terminal carboxylates have $\nu_{asym}COO^-$ and $\nu_{sym}COO^-$ at $1595 \pm 5$ $cm^{-1}$ and $1400 \pm 5$ $cm^{-1}$. The $\Delta\nu$ ($195 \pm 5$ $cm^{-1}$) indicates mode of carboxylate coordination [9, 19] as *syn-syn* chelate. The broad peak at 3440–3460 $cm^{-1}$ for the complexes may be attributed to CH stretch of the aromatic rings.

### 3.2. *Electronic spectra*

Complex **1** possessing cage-like Cu(II) geometry is similar to that in copper(II) acetate monohydrate; the electronic spectra recorded using DMF matches well with cupric acetate. The UV–vis spectra for **1** depict a d-d band at 750 nm along with a sharp band at 260–275 nm corresponding to ligand-centered transition. The peak at 260–275 nm in **1–3** matches well with the peak at 370 nm reported for $[Cu(CH_3COO)_2{\cdot}H_2O]_2$; the shift in their wavelength of 100 nm may be attributed to change in ligand strength. These peaks resemble each other, indicating that this can be attributed to ligand to metal charge transfer mediated through carboxylate oxygen to Cu(II). Visible spectra of **2** and **3** recorded in DMF solvent depict a d–d band at 650 nm. Depending upon the position of the d–d band, the complexes can be arranged in the order of decreasing wavelength **1**(740 nm) > **2** (650 nm) ≈ **3**(648 nm). The change in the position of the d-d band between the complexes **2–3** and **1** can be attributed to change in the geometry [20] (figure 1) of the metal center. The position of the d-d band for **1** represents octahedral geometry and **2** and **3** illustrate five-coordinate, distorted square pyramidal geometry as supported by the crystal structure.

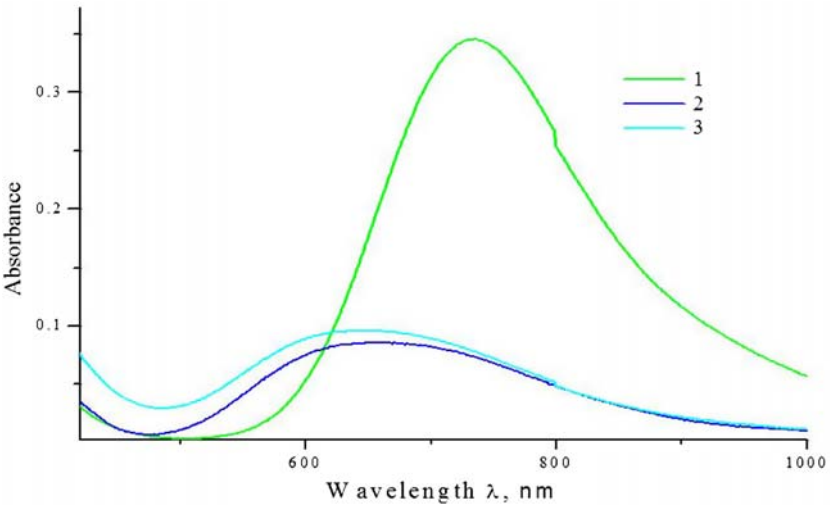


Figure 1. UV–Vis spectra for **1**, **2,** and **3** in DMF.

### 3.3. *Mass spectra*

Mass spectra of **1**, **2,** and **3** are depicted in figure 2. Though the elemental analysis and crystallographic data indicate solvents in **1** and **3**, mass spectral data did not show the presence of solvents, indicating the solvents are labile. The mass value obtained for all these complexes are in accord with formation of dinuclear and monomeric formulas as reported above. In these three complexes, three distinct positive ion peaks were observed. The first and third peak appearing with less intensity represent the hydrogen ion ($M+H^+$) and potassium ion ($M+K^+$) adduct. The dominant middle peak indicates the existence of sodium ($M+Na^+$) adduct for all three complexes. Such observation of positive MS peak obtained with hydrogen, sodium, and potassium ion adduct for the neutral complexes is not uncommon.

### 3.4. *Fluorescence*

Cu(II) complexes are of biochemical interest [21–23] and hence, such complexes with fluorescence are important. Fluorescence spectra recorded in solution for these complexes are depicted in figure 3. The fluorescence spectra measured in DMF ($1\times10^{-5}$ M) at room temperature provide a strong and broad emission at 300–400 nm for **1**, while **2** and **3** give emissions at 400–500 nm ($\lambda_{exc}$, 280 nm). The role of the metal ion is to increase coplanarity and hence, conformational rigidity of the structure which decreases the $\pi$–$\pi^*$ energy gap. Increase in the number of aromatic rings might cause changes in the emission. Thus, the red shift observed among the complexes in the order $1<2<3$ reveals that the emission is caused by $\pi$–$\pi^*$ transition. Fluorescent emission in the visible range exhibited by these complexes suggests that these complexes can act as potential photoactive materials and sensors.

### 3.5. *Crystal structures*

**3.5.1. Crystal structure of 1.** ORTEP diagram of **1** is depicted in figure 4. Summary of the crystallographic data for **1–3** and bond distances and angles of the coordination sphere

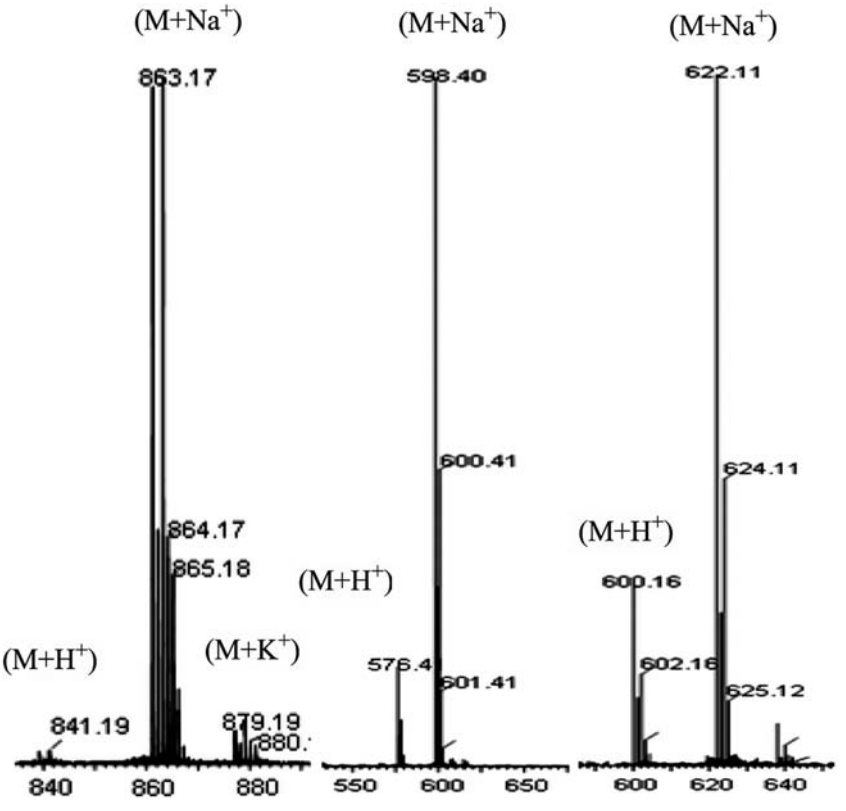


Figure 2. Mass spectra of **1**, **2,** and **3**.

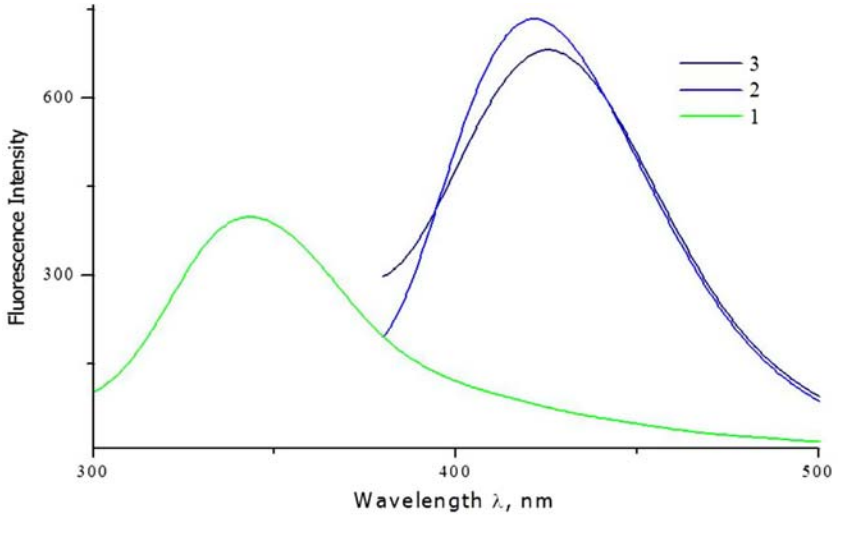


Figure 3. Fluorescence emission spectra for **1**, **2,** and **3** ($\lambda_{ex} = 280$, in DMF, Conc. $1 \times 10^{-5}$ M).

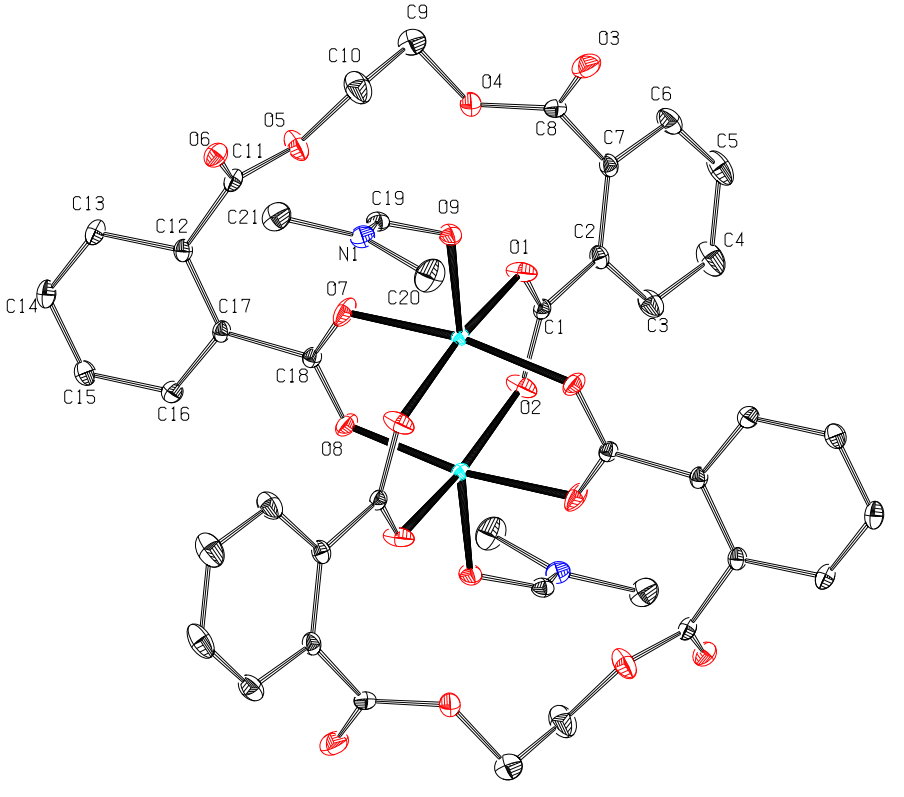


Figure 4. ORTEP diagram of **1** with atom numbering scheme; hydrogens are removed for clarity (40% probability factor for the thermal ellipsoids).

Table 1. Summary of the crystallographic data for **1–3**.

| Complex | **1** | **2** | **3** |
|---|---|---|---|
| Chemical formula | $C_{42}H_{38}Cu_2N_2O_{18}$ | $C_{38}H_{16}Cu_2O_{18}$ | $C_{33}H_{26}Cu\ N_3O_9$ |
| Formula wt. | 985.82 | 887.59 | 672.11 |
| a (Å) | 9.3727(6) | 12.4862(13) | 17.595(11) |
| b (Å) | 10.9760(7) | 14.2327(15) | 11.014(7) |
| c (Å) | 11.2072(7) | 14.1226(15) | 17.595(11) |
| $\alpha$ (°) | 78.5790(10) | 90 | 90 |
| $\beta$ (°) | 76.3630(10) | 108.452(2) | 117.82 |
| $\gamma$ (°) | 73.0790(10) | 90 | 90 |
| $Z$ | 1 | 4 | 4 |
| $V$ (Å$^3$) | 1061.50(12) | 2380.7(4) | 3016(3) |
| Crystal system | Triclinic | Monoclinic | Monoclinic |
| Space group | $P$-1 | $P2_1$/n | $P2_1$/n |
| $\rho_{calcd}$ (g cm$^{-3}$) | 1.542 | 1.607 | 1.480 |
| Abs. coeff. (mm$^{-1}$) | 1.083 | 0.977 | 0.786 |
| Temp. (K) | 100(2) | 100(2) | 293(2) |
| Final R ($F^0{}_2$) | 0.0447 | 0.0494 | 0.0752 |
| Weighted R ($F^0{}_2$) | 0.1153 | 0.1035 | 0.1429 |

Table 2. Selected bond distances and angles for **1–3** with esd's in parenthesis.

| Bond lengths (Å) | | Bond angles (°) | |
|---|---|---|---|
| **1** | | | |
| Cu1–O8$^{\#1}$ | 1.9532(18) | O8$^{\#1}$–Cu1–O1 | 89.55(9) |
| Cu1–O1 | 1.9623(19) | O8$^{\#1}$–Cu1–O7 | 168.34(8) |
| Cu1–O7 | 1.9688(19) | O1–Cu1–O7 | 90.72(10) |
| Cu1–O2$^{\#1}$ | 1.9718(19) | O8$^{\#1}$–Cu1–O2$^{\#1}$ | 89.38(9) |
| Cu1–O9 | 2.1271(18) | O1–Cu1–O2$^{\#1}$ | 168.53(8) |
| Cu1–Cu1$^{\#1}$ | 2.6283(6) | O7–Cu1–O2$^{\#1}$ | 88.05(10) |
| | | O8$^{\#1}$–Cu1–O9 | 96.49(8) |
| | | O1–Cu1–O9 | 99.28(8) |
| | | O7–Cu1–O9 | 94.98(8) |
| | | O2$^{\#1}$–Cu1–O9 | 92.18(8) |
| | | O8$^{\#1}$–Cu1–Cu1$^{\#1}$ | 85.26(6) |
| | | O1–Cu1–Cu1$^{\#1}$ | 85.77(6) |
| | | O7–Cu1–Cu1$^{\#1}$ | 83.14(6) |
| | | O2$^{\#1}$–Cu1–Cu1$^{\#1}$ | 82.76(6) |
| | | O9–Cu1–Cu1$^{\#1}$ | 174.65(5) |
| #1 = $-x+1, -y+2, -z+2$ | | | |
| **2** | | | |
| Cu1–O7 | 1.9084(19) | O7–Cu1–N1 | 171.57(9) |
| Cu1–N1 | 1.977(2) | O7–Cu1–O1 | 94.74(8) |
| Cu1–O1 | 1.9938(19) | N1–Cu1–O1 | 92.04(9) |
| Cu1–N2 | 2.000(2) | O7–Cu1–N2 | 93.24(9) |
| Cu1–O2 | 2.377(2) | N1–Cu1–N2 | 81.47(9) |
| Cu1–C1 | 2.496(3) | O1–Cu1–N2 | 163.65(8) |
| | | O7–Cu1–O2 | 95.36(8) |
| | | N1–Cu1–O2 | 92.37(8) |
| | | O1–Cu1–O2 | 60.11(7) |
| | | N2–Cu1–O2 | 104.95(8) |
| | | O7–Cu1–C1 | 96.43(9) |
| | | N1–Cu1–C1 | 91.96(9) |
| | | O1–Cu1–C1 | 30.48(8) |
| | | N2–Cu1–C1 | 134.17(9) |
| | | O2–Cu1–C1 | 29.63(7) |
| **3** | | | |
| Cu1–O7 | 1.905(4) | O7–Cu1–O1 | 93.66(19) |
| Cu1–O1 | 1.966(5) | O7–Cu1–N1 | 170.43(19) |
| Cu1–N1 | 1.987(5) | O1–Cu1–N1 | 92.1(2) |
| Cu1–N2 | 2.016(5) | O7–Cu1–N2 | 93.3(2) |
| Cu1–C1 | 2.528(7) | O1–Cu1–N2 | 168.7(2) |
| | | N1–Cu1–N2 | 82.3(2) |
| | | O7–Cu1–C1 | 92.18(19) |
| | | O1–Cu1–C1 | 29.66(18) |
| | | N1–Cu1–C1 | 96.6(2) |
| | | N2–Cu1–C1 | 141.1(2) |

#1, #2 denotes the symmetry operator.

is given in tables 1 and 2, respectively. Two symmetrically disposed ligands coordinating through terminal carboxylate form two *[15]*-membered bis-chelate rings on both sides of the M–M axis in **1**. The neutral molecule possesses a center of symmetry passing through the midpoint of Cu1 … Cu1, which is separated by 2.6283(6) Å. The intermetallic distance indicates that **1** is in-line with similar bis-chelate complexes reported recently [13, 14]. Each metal center in the dimer possesses five-coordinate square pyramidal geometry in which four corners of the square base are occupied by oxygens of carboxylate and the axial site is occupied by solvent. The flexible symmetry-related ligands are oriented in

order to coordinate by utilizing O1, O2, O7, and O8 in *syn* mode with an adjacent metal of the dimeric unit and make a slightly distorted square base. The average Cu–O distance of the carboxylate-bridged Cu(11) is 1.9638(18) Å. The square base *cis* angles range from 88.05(10) to 90.72(10)°, while the *trans* angles show considerable deviation (<O(8)–Cu (1)–O(7) = 168.34(8)°,<O(2)–Cu(1)–O(1) = 168.53(8)°) from the ideal value for square planar arrangement, perhaps caused by the Cu … Cu interaction within the dimeric unit. The longer apical coordination is provided by O9 of DMF at Cu(1)–O(9) = 2.1271(18) Å. The carboxylate oxygens of the Cu(II) square base are almost in the plane with Cu(II) sitting 0.158 Å above this plane to make longer apical coordination with DMF. Extensive folding was observed similar to that observed in an isostructural complex with ethanol reported recently [13].

**3.5.2. Crystal structure of 2.** Complex **1**, upon reacting with bpy or phen, gives **2** and **3**. ORTEP diagram of the **2** with an atom numbering scheme is depicted in figure 5. Complex **2** crystallizes in the monoclinic crystal system with $P2_1/n$ space group. Cu(II) possesess a distorted square pyramidal geometry in which the square base is provided by bipyridine nitrogens N1 [Cu1–N1 = 1.977(2) Å] and N2 [Cu1–N2 = 2.000(2) Å] chelated to Cu(II) and terminal carboxylates O7 and O1 [Cu1–O1 = 1.9938(19) Å, Cu1–O7 = 1.9084 (19) Å] attached to the ortho position of the phenyl head group of $L^1$. With O2 [Cu1–O2 = 2.377(2) Å] providing a longer axial coordination, $L^1$ establishes coordination with Cu(II) bidentate at one end while the other end is monodentate, leaving C=O uncoordinated. Bidentate chelate and monodentate coordination from the opposite terminal

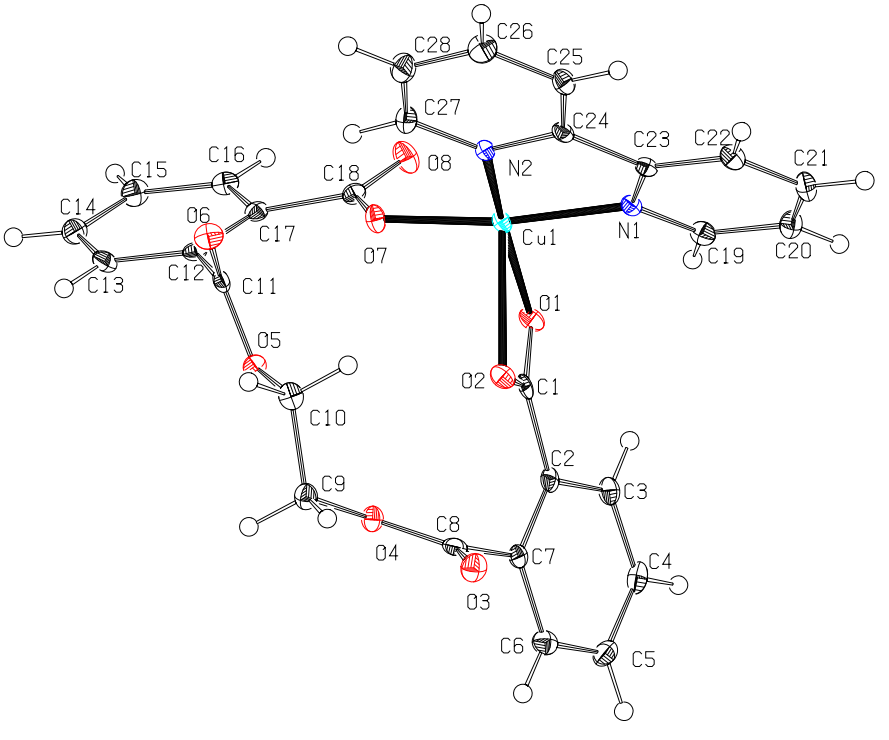


Figure 5. ORTEP diagram of **2** with atom numbering scheme (40% probability factor for the thermal ellipsoids).

of the carboxylate with the same Cu(II) center occurs. The bidentate coordination of one terminal carboxylate is reflected in the angles subtended by O1 and O2 with the metal center, which shows large deviation from ideal. Thus, the axially coordinated O2 has a small angle with O1 (O1–Cu1–O2 = 60.11(7)°) and the *cis* angles subtended by O2 with the surrounding coordinated atoms of Cu(II) range from 92.37(4) to 104.95(8)°. Other *cis* angles of coordinated carboxylate O1 also show slight deviation, 92.04(8) to 94.78(9)°. The deviation on the *trans* angle of O1 involving the metal center and bipyridine nitrogen N2, *i.e.* <O1–Cu1–N2 = 163.65(8)°, indicates slight strain imposed by bidentate coordination of carboxylate. Cu(II) is slightly above (0.078 Å) the square base towards apical O2 to make an effective five coordination. The phenyl ring C2–C7 and C12–C17 of $L^1$ orient almost orthogonal to each other, twisted with 81.91° angle. The aromatic rings on bpy are twisted with respect to each other along the C–C axis by 8.05°, indicating strong chelate coordination of carboxylate O2 with copper, which imposes strain on the terminal phenyl rings. Compound **2** existing with $L^1$ compared to formato and acetato $Cu_2$ complexes, $Cu_2(\mu\text{-HCOO})_4](pymd)_2$, and $[Cu_2(\mu\text{-Ac})_4(pydz)_2]$, reported by Barquin *et al.* [24, 25] indicates paddle wheel geometry; flexibility in the spacer permits Cu–Cu distance of 2.61–2.64 Å in all these complexes.

**3.5.3. Crystal structure of 3.** ORTEP diagram with atom numbering scheme for **3** is depicted in figure 6. Similar to **2**, **3** with 1,10-phenanthroline crystallizes in $P2_1/n$ space group along with one DMF of crystallization and is isostructural. Coordination around Cu(II) can best be described as distorted square pyramidal. N1 [Cu(1)–N(1) = 1.987(5) Å] and N2 [Cu(1)–N(2) = 2.016(5) Å] of phenanthroline and O1 [Cu(1)–O(1) = 1.966(5) Å] and O7 [Cu(1)–O(7) = 1.905(4) Å] of terminal carboxylate oxygens of $L^1$

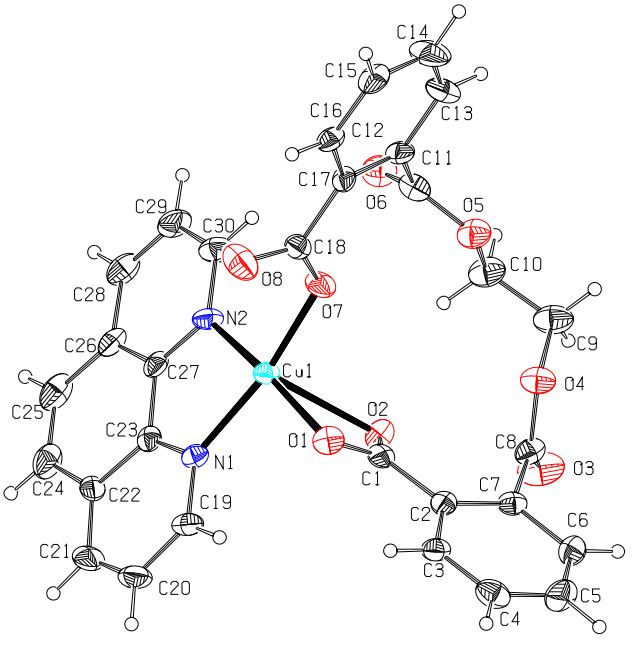


Figure 6. ORTEP diagram depicting **3** with atom numbering scheme (40% probability factor for the thermal ellipsoids).

occupy the corners of the square base with longer apical coordination provided by O2 [Cu(1)–O(2) = 2.446(4) Å]. Similar to **2**, $L^1$ exists in bidentate chelation and monodentate coordination with the same Cu(II). Thus, the symmetrical *syn-syn* arrangement in **1** rearranges into bidentate chelate and monodentate coordination in **2** and **3**. The *cis* angles from 82.3(2) to 93.66(16)° and *trans* angles of 170–169° [<O(7)–Cu(1)–N(1) = 170.43(19)°; <O(1)–Cu(1)–N(2) = 168.7(2)°] of the square base show deviation from ideal planarity. This may be due to strain in the chelate coordination of phenanthroline and bidentate coordination of carboxylate. Cu(II) is slightly above (0.012 Å) the square base towards O2.

Determination of the mode of carboxylate coordination is a challenging assignment in dicarboxylate complexes; the similarity of carboxylate coordination in **2** and **3** indicates detachment of one dicarboxylate from **1** upon bpy/phen interaction. A similar structure reported for Cu(II) oxalate with bpy and phen illustrates that oxalate exists with only chelate coordination. A similar structure reported for malonate [$^{-}$OOC–$CH_2$–COO$^{-}$] dianion and bpy/phen by Zhang *et al*. [26] shows one end of malonate COO with bidentate chelate coordination with one Cu(II), while the COO of the other end is coordinated monodentate with an adjacent Cu(II). Complexes **2** and **3** with bpy and phen are monomeric with dicarboxylate bidentate chelate and monodentate with the same Cu(II). The oxalates reported [27, 28] in $[Cu(II)(oxalate)(bpy)]_n$ and $[Cu(II)(oxalate)(phen)]_n$ provide only bidentate chelate but malonate, longer due to an additonal –$CH_2$– in the spacer, provides both mono and bidentate mode with different Cu(II) centers. In **2** and **3**, $L^1$ has a OOC–$CH_2$–$CH_2$–COO spacer, possessing an additional $CH_2$ and ester groups and $L^1$ gained significant flexibiltiy. This is evident from the twist observed in the spacer moiety as shown in the crystal structure. Thus, the presence of ester and long chain $CH_2$ in the spacer facilitated terminal carboxylate coordinating with the same Cu(II) in both mono and bidentate fashion.

### 3.6. *Supramolecular dimeric association*

Mononuclear **2** and **3** with bpy and phen, respectively, possess strong C–H … O hydrogen bonding [29, 30] and π … π stacking interaction between aryl rings of *N,N* donors, leading to a supramolecularly assembled dimeric association. The free exocyclic oxygen of the terminal carboxylate in both these complexes is involved in strong intermolecular C–H … O interaction, bringing two adjacent monomers into proximity. The CH … O interactions in **2** mediated through H22 [C22–H22 … O2] and H25 [C25–H25 … O2] hydrogens of bpy are 3.205–3.211 Å. A similar interaction in **3** mediated through H24 showing 3.582 Å (C24–H24 … O8 = 3.582 Å,<C24–H24 … O8 = 158.03°) indicates their influence on supramoelcular association. The C–H … O interaction is within the range up to 3.6 Å reported by Nishio *et al*. [29], Desiraju and Steiner [30].

In addition to the C–H … O interaction, π … π stacking interaction also plays a role in the present supramolecular assembly. Distances between the aromatic rings of the bpy/phen moiety of the adjacent monomers, bpy in **2** of 3.88 Å and a closer distance 3.46 Å in **3** indicate weak interaction. The distance measured for π···π stacking interaction in **2** and **3** in the range 3.46–3.88 Å are within the range suggested by Janiak [31] and others [32] of 3.4–4.0 Å. These interactions play roles in the self-assembly of dimers shown in figure 7. The similarity in the orientation of **2** and **3** indicates that dinuclear arrangement is retained even after treating with bpy/phen by rearranging the coordination of COO and appropriately altered by C–H … O/π … π interactions.

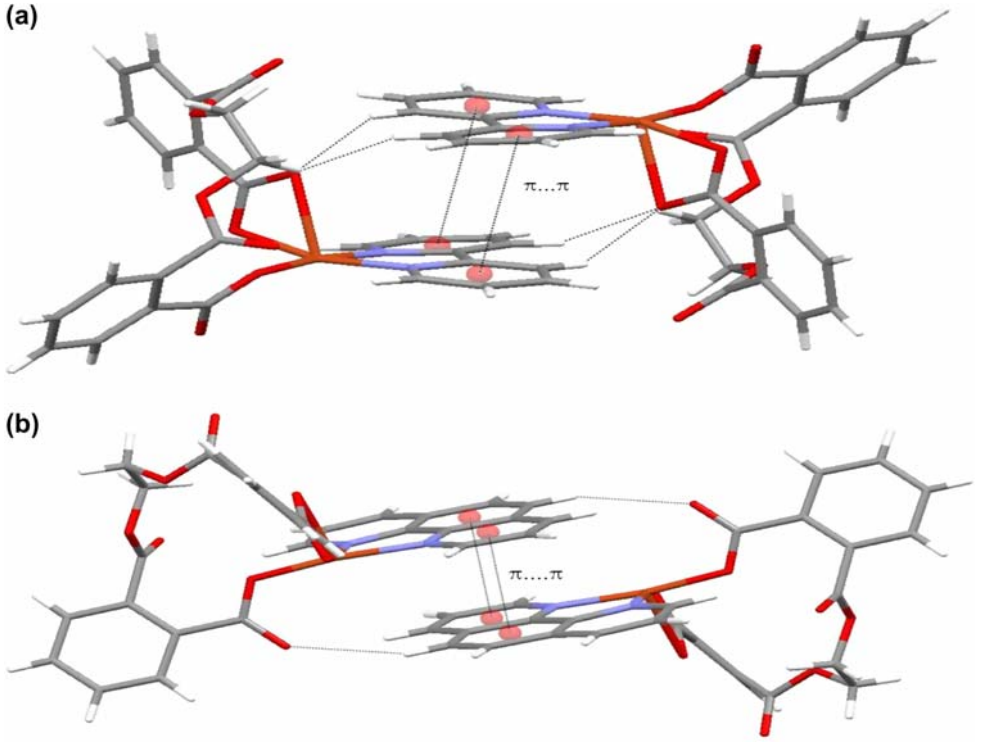


Figure 7. Supramolecular dimeric association of (a) **2** and (b) **3**.

## 4. Conclusions

We have synthesized a dimeric copper(II) tetracarboxylate paddle wheel complex **1** with *[15]*-membered bis-chelate rings symmetrically assembled on both sides of the Cu–Cu–M axis. This symmetrically assembled bis-chelate ring in **1** rearranges into monochelate rings in **2** and **3** by selectively detaching one dicarboxylate upon treating with bipy/phen. Ester oxygens of $L^1$ remain free in all these complexes and terminal carboxylate oxygens show different coordination between **1**, **2,** and **3**. The tetradentate dicarboxylate in **1** provides tridentate coordination in **2** and **3**, leaving one carbonyl ketonic oxygen free. The ester spacer in $L^1$ and the flexibilty for these monodentate and bidentate chelate coordinations with the same Cu(II) center is highlighted. Fluorescent emission exhibited by these complexes in solution suggests that these complexes can act as potential luminescent materials.

## Supplementary data

CCDC 686768, 686769, and 686770 contain the supplementary crystallographic data for this paper. These data can be obtained free of charge via http://www.ccdc.cam.ac.uk/conts/retrieving.html, or from the Cambridge Crystallographic Data Center, 12 Union Road, Cambridge CB2 1EZ, UK; Fax: (+44) 1223-336-033; or E-mail: deposit@ccdc.cam.ac.uk.

## Acknowledgments

The authors PS and PMS are grateful to Department of Science and Technology, New Delhi (India), for financial support vide Project Number SR/S1/IC-19/2005. The author SN is grateful to CSIR funding.

## References

[1] C.N. Rao, S. Natarajan, R. Vaidhyanathan. *Angew. Chem. Int. Ed.*, **41**, 1466 (2004).
[2] R.C. Mehrotra, R. Bohra. *Metal Carboxylates*, Academic Press, London (1983).
[3] B. Bleaney, K.D. Bowers. *Proc. R. Soc. London, Ser. A*, **214**, 451 (1952).
[4] A. Bertini, D. Gatteschi. *EPR of Exchange Coupled Systems*. Chap. 10, Springer Verlag, Berlin (1990).
[5] M. Rusjan, Z. Chaia, O.E. Piro, D. Guillon, F.D. Cukiernik. *Acta Crystallogr.*, **B56**, 666 (2000).
[6] P. Ratnasamy, R. Raja, D. Srinivas. *Philos. Trans. R. Soc. A*, **363**, 1001 (2005).
[7] E.S. Sherman, S.R. Chemler, T.B. Tan, O. Gerlits. *Org. Lett.*, **6**, 1573 (2004).
[8] E.I. Solomon, K.W. Penfield, D.E. Wilcox. *Struct. Bond.*, **53**, 1 (1983).
[9] B.J. Hathaway. In *Comprehensive Coordination Chemistry*, G. Wilkinson, R.D. Gillard, J.A. McCleverty (Eds.), Vol. 5, Chap. 53, p. 558, Pergamon Press, Oxford (1987).
[10] W. Kaim, J. Rall. *Angew. Chem. Int. Ed. Engl.*, **35**, 43 (1996).
[11] M. Melnik. *Coord. Chem. Rev.*, **42**, 259 (1982).
[12] M. Kato, Y. Muto. *Coord. Chem. Rev.*, **92**, 45 (1988).
[13] P. Mosae Selvakumar, E. Suresh, P.S. Subramanian. *Inorg. Chim. Acta*, **361**, 1503 (2008).
[14] P.M. Selvakumar, E. Suresh, S. Waghmode, P.S. Subramanian. *J. Coord. Chem.*, **64**, 3495 (2011).
[15] J. Bickley, R.P. Bonar-Law, M.A. Borrero Martinez, A. Steiner. *Inorg. Chim. Acta*, **357**, 891 (2004).
[16] G.M. Sheldrick. *Acta Cryst.*, **A64**, 112 (2008).
[17] A.L. Spek. *PLATON-97*, University of Utrecht, Utrecht (1997).
[18] Mercury 1.3 Supplied with Cambridge Structural Database, CCDC, Cambridge, UK (2003–2004).
[19] G.B. Deacon, R.J. Phillips. *Coord. Chem. Rev.*, **33**, 227 (1980).
[20] B. Abolmaali, H.V. Taylor, U. Weser. *Struct. Bond.*, **91**, 91 (1998).
[21] A.G. Sykes. *Adv. Inorg. Chem.*, **36**, 377 (1991).
[22] K. Dhara, U.C. Saha, A. Dan, S. Sarkar, M. Manassero, P. Chattopadhyay. *Chem. Commun.*, **46**, 1754 (2010).
[23] Y. He, C. Zhong, Y. Zhou, H. Zhang. *J. Chem. Sci.*, **121**, 407 (2009).
[24] M. Barquin, N. Cocera, M.J. Gonzalez Garmendia, L. Larrinaga, E. Pinilla, M.R. Torres. *J. Coord. Chem.*, **63**, 2247 (2010).
[25] M. Barquin, M.J. Gonzalez Germendia, L. Larrinnaga, E. Pinilla, J.M. Seco, M.R. Torres. *J. Coord. Chem.*, **63**, 1652 (2010).
[26] X.-D. Zhang, Y.-Y. Sun, Z. Zhao, Y.-C. Ma, M.-L. Zhu. *Acta Cryst.*, **C62**, m4–m6 (2006).
[27] J. Kim, U. Lee, B.K. Koo. *Bull. Korean Chem. Soc.*, **31**, 487 (2010).
[28] M. Birzescu, M. Niculescu, R. Dumitru, P. Budrugeac, E. Segal. *J. Therm. Anal. Calorim.*, **94**, 297 (2008).
[29] M. Nishio, M. Hirota, Y. Umezawa. *The C–H ... π Interaction (Evidence, Nature and Consequences)*, Wiley-VCH, New York, NY (1998).
[30] G.R. Desiraju, T. Steiner. *The Weak Hydrogen Bond in Structural Chemistry and Biology*, Oxford University Press Inc., New York, NY (1999).
[31] C. Janiak. *J. Chem. Soc., Dalton Trans.*, 3885 (2000).
[32] P.O. Oguadinma, A. Rodrigue-Whitchel, C. Reber, F. Schaper. *Dalton Trans.*, **39**, 8759 (2010).